

MassChemSite for In-Depth Forced Degradation Analysis of PARP Inhibitors Olaparib, Rucaparib, and Niraparib

Stefano Bonciarelli, Jenny Desantis, Simone Cerquiglini, and Laura Goracci*



Cite This: *ACS Omega* 2023, 8, 7005–7016



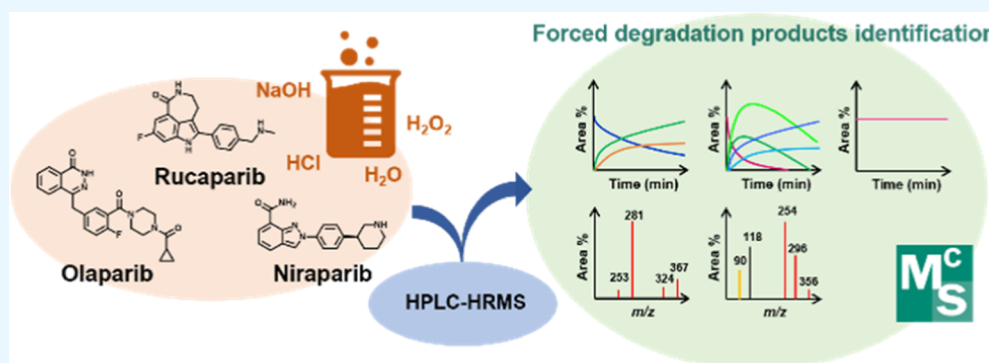
Read Online

ACCESS |

Metrics & More

Article Recommendations

Supporting Information



ABSTRACT: Drugs must satisfy several protocols and tests before being approved for the market. Among them, forced degradation studies aim to evaluate drug stability under stressful conditions in order to predict the formation of harmful degradation products (DPs). Recent advances in LC–MS instrumentation have facilitated the structure elucidation of degradants, although a comprehensive data analysis still represents a bottle-neck due to the massive amount of data that can be easily generated. MassChemSite has been recently described as a promising informatics solution for LC–MS/MS and UV data analysis of forced degradation experiments and for the automated structural identification of DPs. Here, we applied MassChemSite to investigate the forced degradation of three poly(ADP-ribose) polymerase inhibitors (olaparib, rucaparib, and niraparib) under basic, acidic, neutral, and oxidative stress conditions. Samples were analyzed by UHPLC with online DAD coupled to high-resolution mass spectrometry. The kinetic evolution of the reactions and the influence of solvent on the degradation process were also assessed. Our investigation confirmed the formation of three DPs of olaparib and the wide degradation of the drug under the basic condition. Intriguingly, base-catalyzed hydrolysis of olaparib was greater when the content of aprotic-dipolar solvent in the mixture decreased. For the other two compounds, whose stability has been much less studied previously, six new degradants of rucaparib were identified under oxidative degradation, while niraparib emerged as stable under all stress conditions tested.

Drug efficacy is closely related to its physical, chemical, and microbiological stability. The possible formation of degradation products (degradants or DPs) and/or other impurities can influence absorption, distribution, metabolism, and excretion properties and have important repercussions on the safety profile of a drug.¹ Nowadays, forced degradations (also known as stress testing) are routinely performed in pharmaceutical companies in the early stage of the drug development process in order to decrease the risk of failure due to stability problems and to uncover potentially toxic DPs.² Indeed, the investigation of a drug's degradation behavior toward various stressed conditions as well as the characterization of the DP structures is an integral part of the pharmaceutical drug development process.^{3,4} Moreover, it is also pivotal for the design of the manufacturing process, shelf-life determination, formulation, and packaging development. In detail, forced degradation studies aim to accelerate the formation of DPs by exposing the drug to different

physicochemical stress conditions to evaluate its stability and degradation pathways.^{3,5} High-performance liquid chromatography (HPLC) or ultra HPLC (UHPLC) coupled with high-resolution mass spectrometry (HRMS) and/or with UV–vis detectors represent the analytical technique commonly used to evaluate DPs allowing both their structure elucidation and quantification.^{1,6–9} Several regulatory agencies (e.g., FDA, WHO, and ICH) recommend exposure of the drug to acidic, basic, dry heat, oxidation, and light (UV) stress conditions among others.^{10,11} The same agencies indicate in their

Received: December 7, 2022

Accepted: January 20, 2023

Published: February 9, 2023



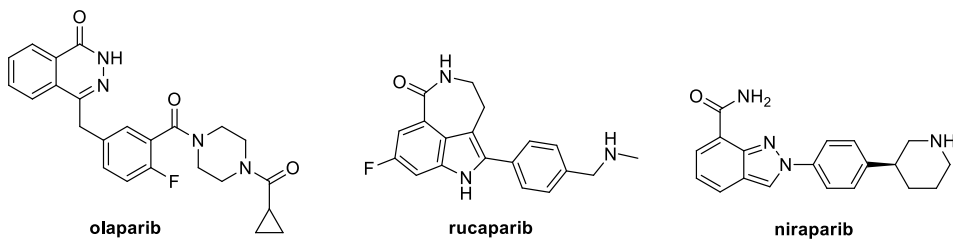


Figure 1. Chemical structures of olaparib, rucaparib, and niraparib.

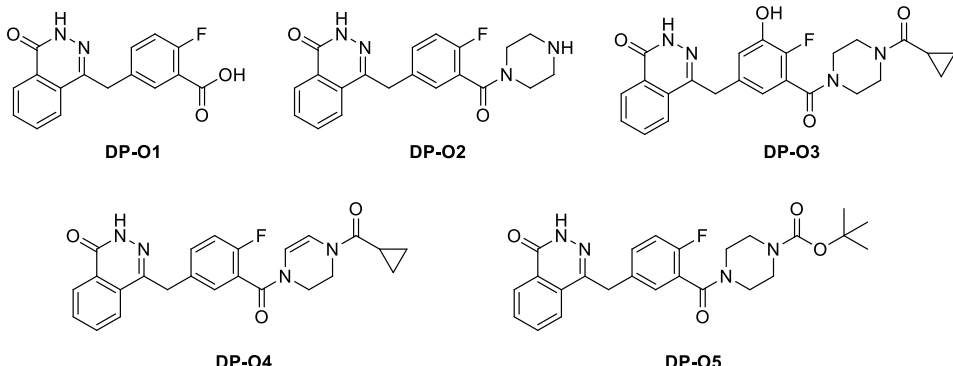


Figure 2. Chemical structures of olaparib DPs reported in the literature.

protocols the ranges of pH, temperature, and maximum exposure time recommended to perform these studies. However, the conditions reported are not stringent. This is because a drug may be more susceptible to acidic hydrolysis than to an oxidative environment and vice versa. Therefore, identifying the optimal conditions for performing degradation tests represents an important task to be defined prior to measurement.^{12,13} In addition to the non-strictly defined experimental conditions, it is worth noting that stress studies are also usually performed by evaluating DP formation at a single time point, making sometimes data interpretation a challenging task. For example, low abundant products could be of uncertain attribution, being close to the noise level, or one product could be a result of a second or a third generation of chemical transformations. Monitoring the degradation process at several time points should be a promising approach to overcome both aforementioned issues, even though data analysis becomes time-consuming and more complex. In this context, MassChemSite (MCS) has been recently reported as a useful tool for the automated analysis of (UHPLC-HRMS)-acquired data providing a rapid and automated structural elucidation of forced DPs.^{14,15} Indeed, its use has been applied to the study of the forced degradation of lansoprazole and allowed automatic identification of the products formed under acidic, basic, neutral, and oxidative stress conditions as well monitoring their kinetic behavior acquiring data at multiple time points.¹⁵ In the present work, we further exploit MCS to study the forced degradation of three poly(ADP-ribose) polymerase (PARP) inhibitors: olaparib, rucaparib, and niraparib (Figure 1).

Olaparib (Lynparza), rucaparib (Rubraca), and niraparib (Zejula) are three FDA approved drugs used for the treatment of ovarian cancer in the patients with hereditary BRCA1 and BRCA2 mutations.^{16–18} They act by inhibiting PARPs, which are a family of enzymes involved in DNA repair through the recognition of DNA damage. The inhibition of these enzymes, which has been elected as a promising anticancer therapeutic

approach, leads to the accumulation of broken single-stranded and double-stranded DNA, thus ultimately culminating in cell death. Despite sharing the same mechanism of action, from the chemical structure point of view as well as their pharmacokinetic properties, these three drugs also have some substantial differences.¹⁹ At the time of our study, a few studies about the forced degradation of olaparib and rucaparib were published,^{20–23} with tests limited to a single time point and in poorly comparable conditions, and sometimes leading to discordant results. In the case of niraparib, to the best of our knowledge, public data about its forced degradation are not publicly available. Therefore, in this work, we decided to study the forced degradation of olaparib, rucaparib, and niraparib under the same stress conditions (basic, acidic, neutral, oxidative environment) at optimized time points and apply the MCS workflow to monitor the compounds' degradation and the formation of DPs over time, as well as to perform the automated structure elucidation of the DPs. Finally, we also tested the effect of different experimental protocols on the final outcomes for olaparib degradation.

RESULTS AND DISCUSSION

Forced Degradation of Olaparib. Previous works have described the forced degradation of olaparib under basic, acidic, neutral, oxidative, dry heat, and photolytic stress conditions.^{20–23} Sample preparation as well as the reaction conditions used to induce the drug's forced degradation change slightly among the cited works. In addition, the DPs observed under the same conditions also differ among the reported studies. For instance, Thummar et al. observed that olaparib was particularly labile to an alkaline environment (0.2 M NaOH, 70 °C for 10 h), leading to two DPs (DP-O1 and DP-O2, Figure 2).²⁰ In contrast, Kallepalli et al. reported that no degradation occurred under basic hydrolysis promoted by 1 M NaOH solution at 80 °C for 1 h.²¹ Different results also emerge from the study of oxidative stress test, where some authors reported an effective degradation while others argue

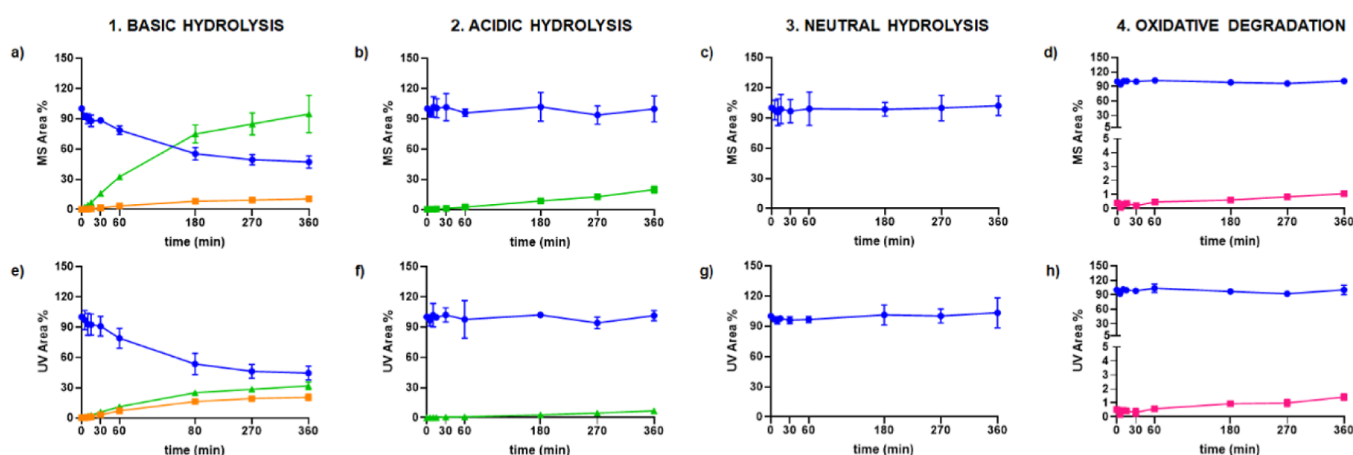


Figure 3. Trend of olaparib and its DPs under the studied stress conditions. Plots of MS area % (top) and UV area % (bottom) vs time for (1) basic hydrolysis (1 M NaOH, 60 °C), (a,e); (2) acidic hydrolysis (1 M HCl, 60 °C), (b,f); (3) neutral hydrolysis (H_2O , 60 °C), (c,g); and (4) oxidative degradation (15% H_2O_2 , 60 °C), (d,h). Olaparib (blue), DP-O1 (orange), DP-O2 (green), and DP-O4 (purple). All the compounds are detected as $[\text{M} + \text{H}]^+$; UV signal is extracted at 254 nm. Data analysis was performed with MCS (version 3.1). Plots prepared with GraphPad Prism (version 8.4.3).

Table 1. Results of the MCS Identification of Olaparib DPs under the Tested Stress Conditions Provided by MS/MS Spectra Matching Comparison^a

Compd	MS/MS spectrum	Basic hydrolysis	Acidic hydrolysis	Neutral hydrolysis	Oxidative stress
DP-O1	<p>Product Spectrum MS2 (+) activ = :ce = 20.0000, Precursor = 299.0833 Z = 1</p> <p>Signal (%) Max: 7.61e-04</p> <p>m/z 159, [Frag]⁺ m/z 253, [Frag]⁺ m/z 281, [Frag]⁺ m/z 103.0540 m/z 131.0517 m/z 159.0548 m/z 205.0755 m/z 233.0708 m/z 253.0771 m/z 281.0723 m/z 299.0830 m/z 300.0830 m/z 323.0708 m/z 350.0771</p>	✓	-	-	-
DP-O2	<p>Product Spectrum MS2 (+) activ = :ce = 20.0000, Precursor = 367.1576 Z = 1</p> <p>Signal (%) Max: 7.39e-05</p> <p>m/z 281, [Frag]⁺ m/z 324, [Frag + H]⁺ m/z 85, [Frag + H]⁺ m/z 253, [Frag]⁺ m/z 85.0764 m/z 100.0764 m/z 150.0764 m/z 200.0764 m/z 250.0764 m/z 253.0775 m/z 281.0728 m/z 324.1154 m/z 367.1577</p>	✓	✓	-	-
DP-O4	<p>Product Spectrum MS2 (+) activ = :ce = 20.0000, Precursor = 433.1681 Z = 1</p> <p>Signal (%) Max: 1.22e-04</p> <p>m/z 281, [Frag]⁺ m/z 365, [Frag + 2H]⁺ m/z 69, [Frag]⁺ m/z 149.0380 m/z 84.0684 m/z 90.0684 m/z 100.0684 m/z 110.0684 m/z 120.0684 m/z 130.0684 m/z 140.0684 m/z 150.0684 m/z 160.0684 m/z 170.0684 m/z 180.0684 m/z 190.0684 m/z 200.0684 m/z 210.0684 m/z 220.0684 m/z 230.0684 m/z 240.0684 m/z 250.0684 m/z 260.0684 m/z 270.0684 m/z 281.0724 m/z 290.0684 m/z 300.0684 m/z 310.0684 m/z 320.0684 m/z 330.0684 m/z 340.0684 m/z 350.0684 m/z 365.1421 m/z 370.0684 m/z 380.0684 m/z 390.1199 m/z 400.0684 m/z 410.0684 m/z 420.0684 m/z 430.2397</p>	-	-	-	✓

^aFragment ions identified as matches and metmatches are reported in red and orange, respectively. DP-O1: m/z 299, $[\text{M} + \text{H}]^+$; DP-O2: m/z 367, $[\text{M} + \text{H}]^+$; DP-O4: m/z 433, $[\text{M} + \text{H}]^+$.

that the drug was stable. A general overview of the already reported studies on olaparib and its related stress impurities is summarized in Table S1 and Figure 2.^{20–23}

Intrigued by the discordant results reported in literature, in this study, we monitored the kinetic evolution (from 0 to 360 min) of the forced degradation of olaparib under basic, acidic,

neutral, and oxidative stress conditions and the elucidation of the DPs was analyzed in depth (Figure 3). Generally, the ideal condition for carrying out stress tests is to promote degradation experiments of the drug in a purely aqueous stock solution. However, when the drug is poorly soluble in water, the use of co-solvent such as acetonitrile (ACN) is

allowed to enhance the solubility.^{2,26} In previous works, different ACN/H₂O ratios have been employed for olaparib forced degradation studies.^{22,23} Here, we decided to prepare a stock solution for olaparib in ACN/H₂O (50:50; v/v %), as previously performed for other drugs (e.g., lansoprazole;¹⁵ cobicistat;²⁷ alvimopan,²⁸ and sumatriptan succinate²⁹). The degradation was then performed in a final solution of ACN/H₂O (25:75; v/v %) after addition of the stress reagent dissolved in water. This experimental procedure permitted a complete substrate dissolution. The samples collected under each stress condition were then neutralized, filtered, and analyzed by UHPLC with online DAD coupled to HRMS. Thus, the obtained raw data files were processed with MCS software. The time evolution of olaparib and its degradants was studied monitoring the MS and UV signals processed by MCS.

As depicted in Figure 3, olaparib (*RT* = 6.89 min, Figure S1) resulted as particularly susceptible to basic hydrolysis (1 M NaOH, 60 °C), where the greater degradation of the substrate was recorded, while less marked degradation of the drug was observed under acid-catalyzed hydrolysis (1 M HCl, 60 °C). In contrast, the degradation of olaparib in neutral solution showed that the drug is stable under all the time points studied. Finally, a slight degradation of olaparib was detected under oxidative stress test (15% H₂O₂ w/w, 60 °C). During analysis, those peaks with sporadic appearance were discarded. The structural identifications of olaparib degradants were performed using the derivatization analysis (untargeted approach) present in MCS.¹⁵ Briefly, after peak detection, MCS performs the identification of given input structure/s (in our case, olaparib, rucaparib, and niraparib) based on the isotopic pattern and fragmentation pattern analysis. Then, MCS uses the initial compound's structure and the reaction given by the user in the processing setting to generate the virtual structures of the products. Finally, in the structure assignment step, the software performs a structure/peak matching based on the *m/z* of the products potentially generated. Afterward, compounds compatible with detected peaks are virtually fragmented to apply a spectral matching approach for further structure identification. Table 1 summarizes the DP identification results for olaparib under the tested stress conditions. In particular, red peaks in the MS/MS spectra represent the fragments that are in favor of the interpretation for the hypothesized product structure (matches), while the cyan peaks represent the fragments that are against the structure interpretation (mismatches). Finally, the orange peaks represent the fragments in favor of interpretation for the selected structure but which appear only in the product spectrum and are not comparable to any fragments in the parent or reference compound (met-matches).¹⁵

MCS revealed the formation of two main DPs, DP-O1 and DP-O2 (Figure 3 and Table 1), under the base-catalyzed hydrolytic condition. DP-O1 (*RT* = 6.23 min, Figure S1) was detected as a pseudo-molecular ion [M + H]⁺ at *m/z* 299.0833. The structure suggested by MCS for this compound derived from the hydrolysis reaction of the amide bond between the phenyl carbonyl group and the nitrogen of the piperazine ring, resulting in the formation of the corresponding benzoic acid derivative. The software identified the fragments at *m/z* 281.0723 (due to loss of H₂O from [M + H]⁺), at *m/z* 261.0644 (loss of HF from *m/z* 281.0723), at *m/z* 253.0771 (loss of CO from *m/z* 281.0723), at *m/z* 233.0708 (loss of HF from *m/z* 253.0771), at *m/z* 159.0548 (loss of C₇H₅FO₂ from

[M + H]⁺), at *m/z* 153.0342 (loss of C₈H₆N₂O from [M + H]⁺), and at *m/z* 133.0289 (loss of C₈H₇FN₂O from [M + H]⁺). No mismatch fragments were reported. DP-O2 (*RT* = 4.25 min, Figure S1) showed a pseudo-molecular ion [M + H]⁺ at *m/z* 367.1576. Its structure derived from the hydrolysis reaction of the amide bond between piperazine and cyclopropane carbonyl group with the formation of the corresponding secondary amine. Furthermore, MCS identified the fragments at *m/z* 324.1154 relating to the fragmentation of the piperazine ring (loss of C₂H₅N from [M + H]⁺), at *m/z* 281.0728 due to the entire cleavage of piperazine from the molecule (loss of C₄H₁₀N₂ from [M + H]⁺), at *m/z* 261.0665 (loss of HF from *m/z* 281.0728), at *m/z* 253.0775 (loss of CO from *m/z* 281.0728), and at *m/z* 85.0764 (piperazine ring [C₄H₉N₂]⁺). No mismatches were detected. Compound DP-O2 was the main product in both basic and acidic degradation (the only degradant observed), although its formation was clearly more favored in an alkaline environment. Finally, only one product (DP-O4) was identified by MCS under an oxidative environment. The pseudo-molecular ion [M + H]⁺ of DP-O4 (*m/z* 433.1681) showed a *m/z* shift of -2 Da compared to olaparib. The structure proposed by MCS for this DP derived from the dehydrogenation of the piperazine ring resulting in the formation of a double bond. Furthermore, the DP-O4 fragmented to give the product ions at *m/z* 391.1199 (loss of C₃H₆ from [M + H]⁺), at *m/z* 365.1421 (loss of C₄H₄O from [M + H]⁺), at *m/z* 281.0724 (loss of C₄H₈N₂ from *m/z* 365.1421), at *m/z* 261.0686 (loss of HF from *m/z* 281.0724), at *m/z* 253.0778 (loss of CO from *m/z* 281.0724), and at *m/z* 69.0341 (2-cyclopropyl ethanal cation, [C₄H₅O]⁺). IUPAC name and mass error (ppm) of the proposed DPs are reported in Table S2.

Because the synthesis of compounds DP-O1 and DP-O2 has been already reported by Menear et al.,³⁰ we decided to synthesize these compounds and analyze them by UHPLC-HRMS with the aim to further validate MCS identification. The *m/z*, *RT*, as well as the fragmentation spectra of synthesized compounds completely overlapped with those of DPs and provided further evidence of the correct MCS identification (data not shown). Overall, the obtained results are in a good agreement with those reported in literature by Thummarr et al.²⁰ Indeed, the authors reported the formation of DP-O1 and DP-O2 in both alkaline and acidic environments and the generation of DP-O4 compound under oxidation.

Solvent Effect Evaluation in Basic Hydrolysis of Olaparib. In forced degradation studies, the drug is usually dissolved in an organic solvent or in an organic/water mixture. The dissolution media generally used is ACN, pure or in aqueous solution. However, the effect that the solvent may have on the degradation is overlooked in these studies. Therefore, taking advantage of the automatic data analysis performed by MCS, in this work, the forced degradation of olaparib under the basic stress condition (1 M NaOH, 60 °C) was also monitored in different ACN/H₂O mixtures. Indeed, basic hydrolysis was the stressful condition in which the drug was more labile and greater degradation was observed (Figure 3). Therefore, this reaction represented an interesting case study to evaluate the effect of the solvent on the degradation rate. In detail, the basic hydrolysis of olaparib conducted in ACN/H₂O (25:75, v/v %), previously described, was compared with the experiments performed in ACN/H₂O (12.5:87.5; v/v %) and H₂O, respectively (Figure 4). The use

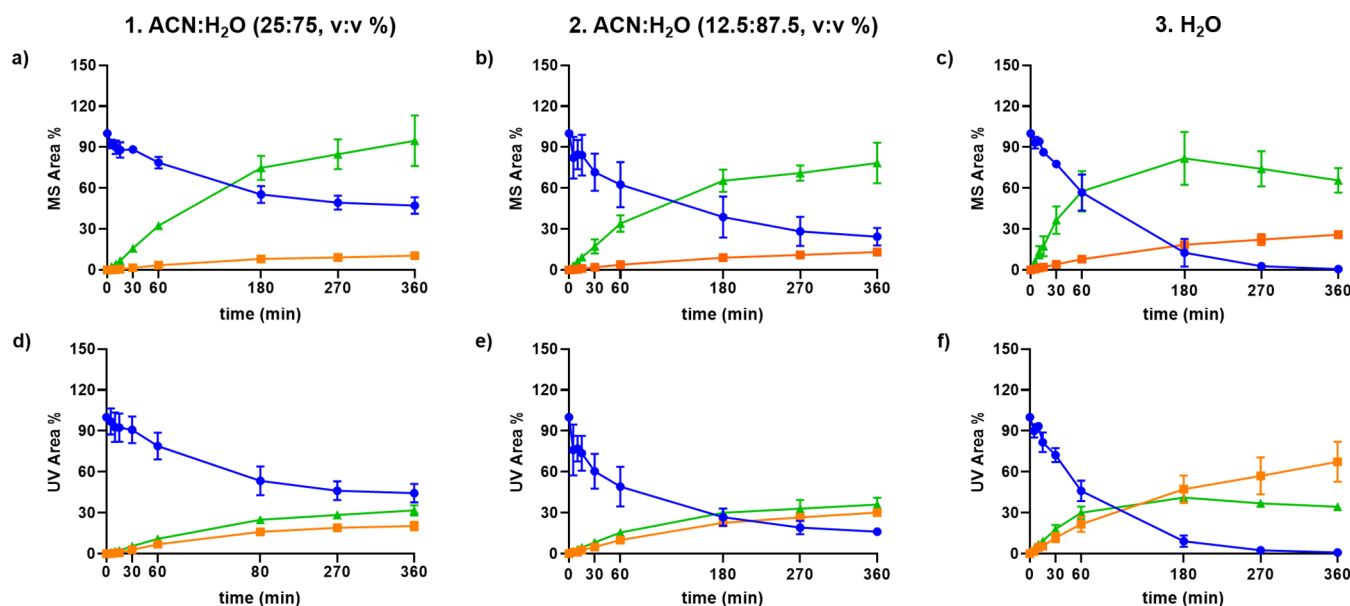


Figure 4. Trend of olaparib and its DPs under the alkaline hydrolysis condition (1 M NaOH, 60 °C). Plots of MS area % and UV area % vs time for the reaction performed in (1) ACN/H₂O (25:75, v/v %), (a,d); (2) ACN/H₂O (12.5:87.5, v/v %), (b,e); and (3) H₂O, (c,f). Olaparib (blue), DP-O1 (orange), and DP-O2 (green). All the compounds are detected as [M + H]⁺; the UV signal is extracted at 254 nm. Data analysis was performed with MCS (version 3.1). Plots prepared with GraphPad Prism (version 8.4.3).

of higher content of ACN in the mixture was also attempted, but in those cases, the formation of non-homogeneous solution due to a salting out effect³¹ did not allow us to follow this condition. The kinetic behavior of olaparib and its degradants was evaluated in the different media monitoring the MS and UV signals provided by the analysis with MCS.

It is commonly accepted that SN2 reactions such as the basic hydrolysis reaction of organic compounds (e.g., esters and amides) promoted by the OH⁻ ion are generally accelerated by using dipolar-aprotic solvents [e.g., ACN, dimethyl sulfoxide (DMSO), dimethylformamide (DMF)].³² This type of reaction mainly proceeds through the formation of a transition state with a more delocalized charge than the starting species. Dipolar-aprotic solvents should solvate the transition state to a greater extent than water and decrease its energy barrier. At the same time, the OH⁻ ion is less solvated than in aqueous solution with increasing its reactivity.³² It has also been reported that the use of mixtures of dipolar-aprotic and protic solvents (e.g., DMSO/H₂O, DMF/H₂O, and ACN/H₂O) increases the rate of basic hydrolysis reactions compared to a purely aqueous medium.³³ In contrast, in this work, the trends obtained by MCS analysis suggest that the base-catalyzed hydrolysis of olaparib is favored in pure water solution. In this condition, the MS area % signal of the substrate decreased by over 40% already after 60 min and the drug was almost completely degraded after 270 min of reaction (MS area % = 2.81). DP-O2 (green) was formed quickly in the first 3 h of reaction, while its signal progressively decreased after that point. In fact, after the complete degradation of olaparib, the alkaline environment may favor the further hydrolysis of DP-O2 to form the DP-O1 product. In addition, less degradation was observed progressively moving toward a higher ACN/H₂O ratio. Indeed, the MS area % signal of olaparib at 360 min resulted as 24.41 and 47.16% in the experiments carried out in ACN/H₂O (12.5:87.5, v/v) and ACN/H₂O (25:75, v/v), respectively. An increase in the reaction rate with the decrease in amount of aprotic dipolar

solvent (ACN) in the organic solvent-water mixture has been already observed for the hydrolysis reactions of esters and other compounds.^{34,35} From a qualitative point of view, this result can be explained by the greater stabilization of the ion pair (Na⁺, OH⁻) by the lone electron pair of the organic solvent (ACN). The higher solvation decreases the reactivity of the OH⁻ ion which is less present in free form in solution.³⁶ Furthermore, another explanation could be the dependence on the dielectric constant of the medium. According to MoKa³⁷ predictions, in a strong basic environment (1 M NaOH, pH = 14) olaparib behaves as a weak acid (predicted pK_a: 11.54, Figure S2) and it is mainly present in dissociated form in the reaction mixture. Amis³⁸ correlated the dependence of the logarithm of the reaction rate ($\ln k$) as a function the reciprocal of the dielectric constant $\left(\frac{1}{\epsilon_r}\right)$ for ion-dipole interactions, eq 1. This relation can be expressed as

$$\ln k = \ln k_{\infty} + \frac{1}{4\pi\epsilon_0} \cdot \frac{z_A \cdot e \cdot \mu_B \cdot N_A}{RT \cdot \epsilon_r \cdot r_{AB}^2} \quad (1)$$

where k_{∞} is the rate constant in a medium with infinite value of electric permittivity, ϵ_0 is the dielectric constant in vacuum, $z_A \cdot e$ is the charge of the ion A, μ_B is the dipole moment of a dipole B at the distance r_{AB} , and N_A is Avogadro's number. Using the equation, $\ln k$ varies linearly as a function of $\frac{1}{\epsilon_r}$ with a slope that depends on the value of $z_A \cdot e$. The slope is negative if $z_A \cdot e$ is a negative and a positive slope if $z_A \cdot e$ is positive. In the case study, the ion OH⁻ has a negative charge equal to that a single electron (-1.602×10^{-19} C) and therefore $\ln k$ proportionally increases with the ϵ_r of the medium moving from ACN/H₂O mixture to a purely water solution. Based on the dielectric constants' values (Table S3), the $\ln k$ of the basic hydrolysis of olaparib increases with the extent of aqueous solvent used and reaches its higher value in only water for the set of experiments studied. In conclusion, although ACN/H₂O mixtures are often used to avoid solubility issues in water, the use of a larger

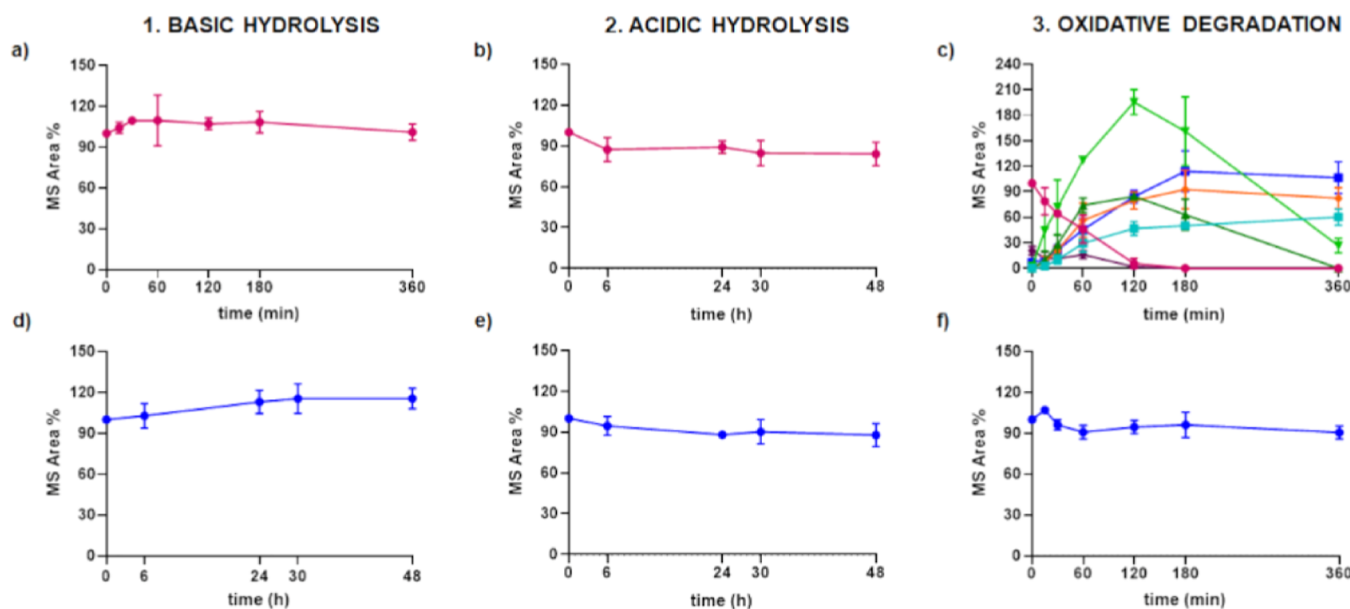


Figure 5. Trend of rucaparib, rucaparib DPs, and niraparib under the studied stress conditions. Plot of MS area % vs time for (1) basic hydrolysis (1 M NaOH, 60 °C) of rucaparib (a) and niraparib (d); (2) acidic hydrolysis (1 M HCl, 60 °C) of rucaparib (b) and niraparib (e); and (3) oxidative degradation (15% H₂O₂, 60 °C) of rucaparib (c) and niraparib (f). Rucaparib (purple), DP-R1 (violet), DP-R2 (light green), DP-R2' (dark green), DP-R3 (cyan), DP-R3' (blue), DP-R4 (orange), and niraparib (blue). All the compounds are detected as [M + H]⁺; UV signal is extracted at 254 nm. Data analysis was performed with MCS (version 3.1). Plots prepared with GraphPad Prism (version 8.4.3).

percentage of water could sometimes increase the amount of DPs formed, simplifying their experimental detection. Additional studies are also in progress to evaluate the effect of the ionization state of a drug in the forced degradation in basic hydrolysis conditions.

Forced Degradation of Rucaparib and Niraparib. At the time of this paper preparation, only two recent publications on the degradation of rucaparib had been reported,^{24,25} while niraparib forced degradation remains an unknown topic. In detail, only the work published by Palakeeti et al.²⁴ was focused on the structure elucidation of the DPs by HPLC-HRMS (Figure S3), while Suchitra and Battu²⁵ studied the forced degradation of rucaparib using a reverse phase-HPLC method with online DAD detector. As for olaparib, the sample preparation, as well as the reaction conditions used to induce the drug degradation, change slightly between the two studies (Table S4). However, both the articles reported that the drug was mainly degraded under alkaline, acidic, and oxidative conditions compared to the other stress conditions. Therefore, in this work, we also investigate the forced degradation of these two PARP inhibitors under alkaline (1 M NaOH, 60 °C), acidic (1 M HCl, 60 °C), and oxidative (15% H₂O₂, w/w, 60 °C) conditions in ACN/H₂O (25:75, v/v %) as described above for olaparib. The acidic reactions were performed over 48 h, while the oxidative degradation was evaluated for up to 360 min for both drugs. In contrast, the alkaline condition was monitored for 360 min and 48 h for rucaparib and niraparib, respectively. Analogously to olaparib stress tests, the samples collected under each stress condition were neutralized, filtered, and analyzed by UHPLC with online DAD coupled to HRMS. It allowed the evaluation of the relative stability of the two drugs under the same reaction conditions. The time evolution of rucaparib, niraparib, and detected DPs is reported in Figures 5 and S4.

No degradation of rucaparib and niraparib was detected under basic conditions using a 1 M NaOH solution. The signal

of the drugs varied slightly in the different time-points. However, it was not possible to study the alkaline degradation of rucaparib for a reaction time greater than 360 min due to the formation of a suspension within the solution. Additional investigations were carried out to identify the precipitate. Indeed, after filtration and further UHPLC-HRMS analysis, the precipitated compound was identified as rucaparib and confirmed by comparison with drug pure standard. Rucaparib was also detected in the filtered solution. No signal corresponding to other compounds was detected (data not shown). No degradation was observed for both rucaparib and niraparib when the hydrolysis reaction was promoted by a 1 M HCl solution. The two PARP inhibitors are therefore stable under hydrolytic conditions (alkaline and acid) at 60 °C. On the other hand, the oxidative degradation of the two drugs showed different results. Rucaparib (purple, *RT* = 9.16 min) exhibited low chemical stability to the oxidative condition, while niraparib was found unreactive. The MS area % value of rucaparib was already half of its initial value after 60 min and it decreased close to zero at 180 min of reaction. A representative sample chromatogram of forced oxidative degradation of rucaparib, is shown in Figure S5. The automated analysis performed using the derivatization analysis (untargeted approach) included in MCS allowed the identification of six main DPs of rucaparib under the oxidative condition (Table 2). The least abundant, DP-R1 (violet in Figure 5c, *RT* = 7.20 min), showed a pseudo molecular ion [M + H]⁺ at *m/z* 340.1452, resulting in mass increment of +16 Da compared to rucaparib. The software identified the fragments at *m/z* 309.1035 (due to loss of CH₃NH₂ from [M + H]⁺) and at *m/z* 280.0774 (loss of CH₂NH from *m/z* 309.1035) as matches. In addition, seven fragments were identified as metmatches at *m/z* 311.1053 (loss C₂H₅• from [M + H]⁺), at *m/z* 292.0883 (loss C₂H₈O from [M + H]⁺), at *m/z* 281.1062 (loss of C₂H₅NO from [M + H]⁺), at *m/z* 224.0872 (loss C₂H₃NO from *m/z* 281.1062), at *m/z* 203.0596 (loss of

Table 2. Results of the MCS Identification of Rucaparib DPs under the Tested Stress Conditions Provided by MS/MS Spectra Matching Comparison^a

Compd	MS/MS spectrum	Basic hydrolysis	Acidic hydrolysis	Oxidative stress
DP-R1	<p>Product Spectrum MS2 (+) activ = :ce = [20 - 35], Precursor = 340.1452 Z = 1</p> <p>Chemical structure of rucaparib derivative DP-R1: A tricyclic indole derivative with a benzyl group at the 2-position and a hydroxyl group at the 4-position.</p> <p>Mass spectrum showing Signal (%) vs m/z. Key peaks labeled: 65.0380, 91.0541, 131.0487, 165.0585, 203.0596, 224.0872, 252.0791, 280.0774, 309.1035.</p>	-	-	✓
DP-R2 and DP-R2'	<p>Product Spectrum MS2 (+) activ = :ce = [20 - 35], Precursor = 356.1404 Z = 1</p> <p>Chemical structure of rucaparib derivative DP-R2: Similar to DP-R1, but with a hydroxyl group at the 2-position instead of the 4-position.</p> <p>Mass spectrum showing Signal (%) vs m/z. Key peaks labeled: 90.0465, 116.0486, 235.0792, 249.0943, 263.0739, 279.0690, 292.1005, 308.0952.</p>	-	-	✓
DP-R3 and DP-R3'	<p>Product Spectrum MS2 (+) activ = :ce = [20 - 35], Precursor = 356.1405 Z = 1</p> <p>Chemical structure of rucaparib derivative DP-R3: Similar to DP-R1, but with a hydroxyl group at the 2-position and a hydroxymethyl group at the 4-position.</p> <p>Mass spectrum showing Signal (%) vs m/z. Key peaks labeled: 90.0465, 118.0415, 226.0663, 254.0608, 278.0602, 296.0706, 325.0978, 356.1372.</p>	-	-	✓
DP-R4	<p>Product Spectrum MS2 (+) activ = :ce = [20 - 35], Precursor = 372.1354 Z = 1</p> <p>Chemical structure of rucaparib derivative DP-R4: Similar to DP-R1, but with hydroxyl groups at both the 2 and 4 positions.</p> <p>Mass spectrum showing Signal (%) vs m/z. Key peaks labeled: 90.0467, 118.0414, 148.0754, 225.0582, 253.0530, 279.0691, 308.0954, 324.0892, 341.0925.</p>	-	-	✓

^aFragment ions identified as matches are reported in red, while metmatch ions in orange. DP-R1: m/z 340, $[M + H]^+$; DP-R2: m/z 356, $[M + H]^+$; DP-R3: m/z 356, $[M + H]^+$; DP-R4: m/z 372, $[M + H]^+$.

$C_8H_{11}NO$ from $[M + H]^+$, at m/z 165.0585 (loss of $C_8H_3O^+$ from m/z 280.0774), and at m/z 91.0541 ($C_7H_7^+$). No mismatch fragments were reported. Two more abundant DPs, namely, DP-R2 and DP-R3, were also found by MCS. DP-R2 (light green in Figure 5c, RT = 7.40 min) resulted in the main DP after 120 min of reaction with the highest MS area % detected. Then, its signal decreased significantly until it reached a MS area % value of 26.61 at 360 min. This DP showed a pseudo-molecular ion $[M + H]^+$ at m/z 356.1404, resulting in a m/z shift of +32 Da compared to rucaparib that may suggest an oxidation via the addition of two oxygen atoms.

Using the processing parameters specifically set in this work (Tables S6 and S7), MCS identified the fragment ions at m/z

325.0982 (match), at m/z 308.0952 (metmatch), at m/z 292.1005 (metmatch), at m/z 263.0739 (metmatch), at m/z 235.0792 (match), at m/z 234.0713 (metmatch), and at m/z 116.0486 (metmatch). However, the structure proposed (with the specific settings used) derives from a gem-hydroxylation of the benzylic methylene group that under the oxidative condition employed (15% H_2O_2) could lose a water molecule to form a more stable amide, thus resulting in an unexpected identification to be further investigated. MCS suggested this structure as a result because the hydroxylation reaction was allowed at all the carbon atoms of the rucaparib structure during the in silico product generation step, setting the number of iterations of hydroxylation equal to three to generate DPs

derived from a double or triple oxidation. More details have been already discussed previously by Bonciarelli et al.¹⁵ In contrast, the formation of **DP-R3** (blue in Figure 5c, $RT = 6.90$ min) was less pronounced at the first stages of reaction. Nevertheless, it turned out to be the most abundant DP (relative quantification) at the end of the oxidation process. The compound **DP-R3** was detected at m/z 356.1405 as a pseudo-molecular ion $[M + H]^+$. The software-driven analysis allowed us to identify the fragments at m/z 325.0978 (loss of CH_3NH_2 from $[M + H]^+$), at m/z 308.0717 (loss of NH_3 from m/z 325.0978), at m/z 296.0706 (loss of CH_2NH from m/z 325.0978), at m/z 280.0742 (loss of CH_3NO from m/z 325.0978), at m/z 268.0755 (loss of CO from m/z 296.0706), and at m/z 254.0608 (loss of CH_2 from m/z 268.0775) as matches. Nine metmatches were also detected at m/z 297.1013 (loss of $\text{C}_2\text{H}_5\text{NO}$ from $[M + H]^+$), at m/z 283.0867 (loss of $\text{C}_3\text{H}_7\text{NO}$ from $[M + H]^+$), at m/z 278.0605 (loss of $(\text{NH}_3 + 2\text{H})$ from m/z 297.1013), at m/z 250.0660 (loss of CO from m/z 278.0605), at m/z 236.0505 (loss of H_2O from m/z 254.0608), at m/z 226.0659 (loss of CO from m/z 254.0608), at m/z 107.0489 ($\text{C}_7\text{H}_7\text{O}^+$), at m/z 90.0465 (C_7H_6^+), and at m/z 89.0389 (C_7H_5^+). No mismatches were reported. In addition, the chromatograms of **DP-R2** and **DP-R3** showed two less abundant shoulder peaks eluting before the main compounds (Figure S6), respectively. The two products, namely, **DP-R2'** (dark green in Figure 5c, $RT = 7.33$ min) and **DP-R3'** (cyan in Figure 5c, $RT = 6.80$ min) showed the same MS/MS spectrum compared to **DP-R2** and **DP-R3** (see Table 2) as well as the same time evolution behavior, respectively. Unfortunately, the optimization of chromatographic conditions did not allow the complete baseline separation of peaks corresponding to these species. While MCS provided only a potential identification for **DP-R2** and **DP-R2'**, **DP-R3** and **DP-R3'** were recognized by the software as two isomers formed by an hydroxylation at position C-7 or C-9 of the rucaparib dihydro-azepino[5,4,3-cd]indolone scaffold combined with an additional hydroxylation at the benzylic methylene group. In addition, **DP-R2'** emphasized the importance of performing the degradation test following the evolution of the reactions over all the exposure time of the forced experimental conditions. As reported in Figure 5c, the compound showed a good temporal profile with the increase in MS signals until 120 min of reaction. However, at the beginning and at the end of the reaction, both its MS area % and UV area % had a zero value (Table S5). Therefore, if an operator had performed the MS analysis only at the end of the studied reaction (here 360 min), he would not have been able to detect **DP-R2'**, losing information about the degradation of the investigated drug. MCS detected a further DP, **DP-R4** (orange in Figure 5c, $RT = 8.48$ min), observed at m/z 372.1354 as a pseudo-molecular ion $[M + H]^+$. The m/z shift of +48 Da suggested an oxidation product formed via the addition of three oxygen atoms. MCS identified as matches the fragments at m/z 341.0925 (loss of CH_3NH_2 from $[M + H]^+$), at m/z 270.0556 (loss of $\text{C}_3\text{H}_5\text{NO}$ from m/z 341.0925), at m/z 267.0675 (loss of $\text{C}_3\text{H}_9\text{N}_2\text{O}_2$ from $[M + H]^+$), and at m/z 253.0530 (loss of CH_2 from m/z 267.0675). In addition, 10 fragment ions were detected as metmatches at m/z 324.0892 (loss of OH^\bullet from m/z 341.0925), at 308.0954 (loss of O from m/z 324.0892), at m/z 296.0944 (loss of CO from m/z 324.0882), at m/z 294.0539 (loss of CH_5NO from m/z 341.0925), at m/z 242.0614 (loss of CO from m/z 270.0556), at m/z 119.0729 ($\text{C}_8\text{H}_9\text{N}^+$), at m/z 107.0499 ($\text{C}_7\text{H}_7\text{O}^+$), at

m/z 105.0327 ($\text{C}_7\text{H}_5\text{O}^+$), at m/z 90.0467 (C_7H_6^+), and at m/z 89.0390 (C_7H_5^+). **DP-R4** was relatively less abundant compared to **DP-R3**, while it exhibited a MS area % higher than **DP-R2** at the end of the reaction, resulting in the second major DP of rucaparib under oxidative degradation (relative quantification). IUPAC name and mass error (ppm) of the identifications proposed by MCS for rucaparib DPs are reported in Table S2. It is worth noting that, to the best of our knowledge, all the six DPs of rucaparib formed by the oxidative stress reaction and described above are reported for the first time in this study. Furthermore, the analysis with MCS allowed us to detect another compound at m/z 309.1039 ($RT = 9.86$ min) whose signal decreases over the time (Figures S7 and S8). The compound was previously reported in Palakeeti et al.²⁴ as an impurity (Imp-C, Figure S3) of rucaparib detected under the oxidative stress test. A summary of the behaviors of olaparib, rucaparib, and niraparib and their corresponding DPs under the studied condition is shown in Table S5.

Additional Manually Investigated Oxidative Degradation Products of Rucaparib. The identification of **DP-R2** and **DP-R2'** as a gem-hydroxylated products described above (Table 2) led us to manually re-inspect the MS/MS spectra of the rucaparib DPs. In this context, an evident difference in the fragmentation fingerprint emerged comparing the four tandem mass spectra at low m/z values (Table 2). In detail, the fragmentation of **DP-R1**, **DP-R3**, **DP-R3'**, and **DP-R4** generated the characteristic product ions at m/z 90 and at m/z 91, while this ion was practically absent in the spectra of **DP-R2** and **DP-R2'** (Table 2). The previous MCS analysis associated these two fragments with a benzyl ion (Figure 6).

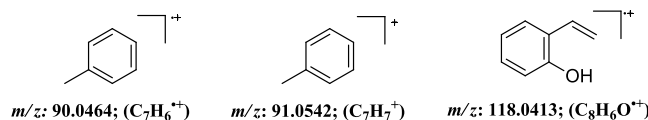


Figure 6. Structure characterization suggested by MCS for product ions at m/z 90 and m/z 91 and our proposed structure for the fragment at m/z 118. Theoretical m/z value and chemical formula are reported for each product ion.

Similarly, the product ion at m/z 118 was found in **DP-R3**, **DP-R3'**, and **DP-R4** MS/MS spectra only, confirming a common substructure for these products but lacking in **DP-R2** and **DP-R2'** (Table 2). Intriguingly, no automated structure interpretation was provided by MCS for the product ion at m/z 118 at least with the used settings (Tables S6 and S7); thus, we attempted to propose a hypothesis about the nature of this ion. The structure representation of fragment at m/z 90 and m/z 91 provided by MCS as well as our proposed structure of product ion at m/z 118, are showed in Figure 6.

The occurrence of fragment m/z 118 may first suggest that the oxidation in **DP-R3**, **DP-R3'**, and **DP-R4** could occur at the benzene ring of rucaparib. On the other hand, the simultaneous presence of the product ion at m/z 90 in their spectra was in contrast with this thesis. Therefore, the structures we hypothesized for **DP-R3** and **DP-R3'** resulted from a first C-hydroxylation in position C-3 of the dihydro-azepino[5,4,3-cd]indolone scaffold and a second C-hydroxylation occurring in one of the two fluorine vicinal positions (i.e., C-7, C-9) as suggested before by MCS. The provided structures may explain the formation of the two observed

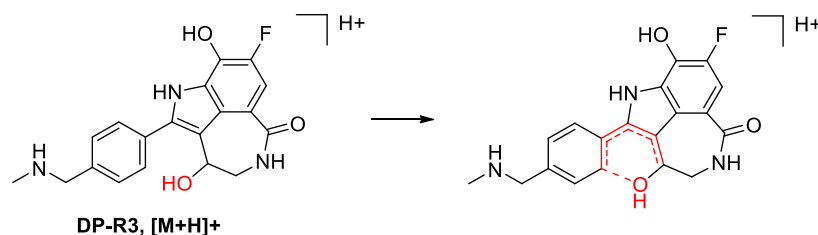


Figure 7. Hypothesized intramolecular rearrangement occurring during fragmentation in DP-R3, DP-R3', and DP-R4 compounds. DP-R3 used as example in the scheme.

isomers without complete peak base separation. Based on this hypothesis, the generation of the ion at m/z 118 could be the result of an intramolecular rearrangement occurring during fragmentation, though the migration of the oxygen in position C-3 of the dihydro-azepino[5,4,3-cd]indolone scaffold to the meta-position of the neighboring N-methylbenzylamine moiety (Figure 7).

A similar intramolecular rearrangement occurring during fragmentation events has been previously described by Grützmacher³⁹ as a common reaction for aromatic radical cations in which a nucleophilic group located in suitable positions can attack the ionized benzene ring intramolecularely.

Regarding DP-R4 elucidation, we hypothesized that this compound could form by further oxidation of DP-R3 and DP-R3' in positions C-7 and C-9 of the dihydro-azepino[5,4,3-cd]indolone scaffold, respectively, as already suggested by MCS. The MS/MS spectrum of DP-R2 and DP-R2' was characterized by intense fragment ions at high values of m/z , while the peculiar fragment ions at m/z 90, m/z 91, and m/z 118 were absent or detected with very low abundance (Table 2). In this case, the oxidation process may lead to the formation of a DP via the addition of two oxygens in the structure of rucaparib: one in the benzyl moiety (absence of both ions at m/z 90 and 91) and another one in the indole substructure (absence of m/z 118). As for DP-R3 and DP-R3', an oxidation in positions C-7 and C-9 of the dihydro-azepino[5,4,3-cd]indolone scaffold was in agreement with the observed co-eluting peaks related to DP-R2 and DP-R2'. Finally, DP-R1 as DP-R2 and DP-R2' did not show the fragment at m/z 118, suggesting a hydroxylation product of rucaparib with no-oxygen addition in position C-3 of the dihydro-azepino[5,4,3-cd]indolone scaffold. In addition, the product ion at m/z 91.0541 related to the benzyl cation represented the most intense fragmentation in the MS/MS spectrum of the compound, suggesting that the oxidation probably did not involve the benzene ring. The structures of the DPs of rucaparib hypothesized after the analysis of MCS and further manual investigation of MS/MS spectra are provided in Figure 8.

Although our supposition for DP-R1 could result in the formation of two isomers as previously observed for the compounds DP-R2 and DP-R3, the low intensity of the DP-R1 compound could influence the detection of the possible less abundant species.

Manual characterization of product ions detected in the MS/MS spectra of rucaparib DPs is provided in the Supporting Information. IUPAC name and mass error (ppm) of the identifications proposed by manual investigation for rucaparib DPs are reported in Table S2.

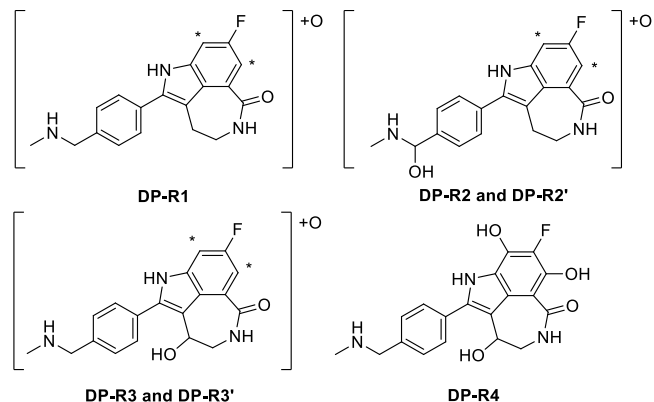


Figure 8. Structure representation of the DPs of rucaparib formed under oxidative stress condition hypothesized after MCS analysis and further manual investigation of the detected fragmentation pattern. (*) indicates the possible oxidation positions in DP-R1, DP-R2 and DP-R2', and DP-R3 and DP-R3' structures.

CONCLUSIONS

In forced degradation studies, the detection and characterization of DPs can be hampered by their low abundance and by the intrinsic complexity of manual inspection of a large amount of data acquired by modern LC–MS instrumentations. MCS was recently reported as a useful informatics tool for data analysis and for the automated identification of DPs, providing a structural characterization of the compounds under study. In the present work, MCS was used to study the forced degradation of three drug PARP inhibitors: olaparib, rucaparib, and niraparib. While the degradation of olaparib was already studied in similar conditions and with discordant findings, only two studies about forced degradation of rucaparib were published, and data about the DPs of niraparib were not publicly available. Analysis with MCS confirmed the formation of two main degradants for olaparib under basic hydrolysis conditions (DP-O1 and DP-O2) and showed a less pronounced degradation in the other conditions studied (acidic, neutral, and oxidative). We also proved that the selection of the reaction solvent and the experimental protocol can influence the extent of degradation. Particularly, the degradation of olaparib under basic hydrolysis was more pronounced when the content of water as a protic solvent in the mixture is increased, although basic hydrolysis reactions of esters and amides are generally accelerated by using dipolar-aprotic solvents. The stress studies on rucaparib revealed an extended degradation of the drug under the oxidative condition applied. The assisted analysis with MCS revealed the formation of six rucaparib DPs, namely, DP-R1, DP-R2, DP-R2', DP-R3, DP-R3', and DP-R4) not reported in literature before, and proposed structures are discussed for

the first time in the present work. In addition, a fragmentation derived from an intra-molecular rearrangement occurring during fragmentation events was hypothesized to explain the observed product ion at m/z 118 detected in the MS/MS spectra of **DP-R3**, **DP-R3'**, and **DP-R4**. In this regard, we proposed a subsequent manual structure elucidation of the rucaparib DPs which included the aforementioned hypothesized fragmentation. The forced degradation of niraparib revealed the stability of the drug under the stress conditions studied. Finally, we can conclude that monitoring the kinetic profile in forced degradation studies following the variation of MS and/or UV signals over time facilitates the detection of DPs and that software for automated structure elucidation like MCS represent powerful tools to reduce time for LC–MS/MS and UV data interpretation, allowing the scientist to focus on challenging assignations only, if not automatically detected.

The potential use of other informatic solutions for automated structure elucidation in forced degradation studies is also planned in the future to reveal advantages and limitations of each of them.

METHODS

Chemicals and Reagents. Olaparib, rucaparib, and niraparib were bought from Biosynth Carbosynth, UK. Their purity (>98%) was confirmed by UHPLC-DAD analysis. Compounds **DP-O1** and **DP-O2** were synthesized as previously reported.³⁰ UHPLC grade water and ACN were purchased from Merck (Italy), while UHPLC grade formic acid (FA) was bought from Avantor (Italy). Analytical grade lab reagents, such as manganese(IV) oxide (MnO_2), sodium hydroxide (NaOH) pellets, hydrochloric acid (HCl), and 30% (w/w) hydrogen peroxide (H_2O_2), were acquired from Merck (Italy).

Instrumentation. Analysis was performed on an Agilent 1290 Infinity Series UHPLC System (Agilent Technologies, Santa Clara, CA, USA) with an online 1290 Infinity Series DAD detector (Agilent Technologies) coupled to a Q-TOF 6540 high-resolution mass spectrometer (Agilent Technologies). The instrumentation was controlled by Agilent Mass-Hunter B.05.01 software.

UHPLC-ESI-HRMS Conditions. The chromatographic separation of olaparib, rucaparib, and niraparib was performed by using a Luna Omega C-18 Polar column (1.6 μm , 100 \times 2.1 mm, Phenomenex) with a gradient mobile phase of (0.1%, v/v) FA (eluent A) and ACN + FA (0.1%, v/v) (eluent B). The following gradient was applied to achieve the compounds separation. Olaparib: 10% B at 0 min, 10% B at 3 min, 75% B at 12 min, 75% B at 16 min. Rucaparib: 0.5% B at 0 min, 0.5% B at 1 min, 30% B at 13 min, 95% B at 17 min, 95% B at 18 min. Niraparib: 10% B at 0 min, 10% B at 3 min, 95% B at 12 min, 95% B at 16 min. The flow rate was set to 0.6 mL min⁻¹, the column temperature was 40 °C, and the injection volume was 2 μL for both olaparib and niraparib samples, while it is 5 μL for rucaparib. Each gradient program includes 2 min of post-time to return to the initial chromatographic conditions.

The mass spectrometer condition was the same described in Bonciarelli et al.¹⁵ with minor modifications. Briefly, the mass spectrometer analysis was performed in positive ionization mode (ESI+) in the mass range from 100 to 1700. The operating source conditions were as follows: gas temperature 350 °C, drying gas flow 9 l min⁻¹, nebulizer 35 psig, sheath gas temperature 400 °C, sheath gas flow 9 l min⁻¹, capillary voltage 4000 V, nozzle voltage 0 V, fragmentor 120 V, skimmer 65 V,

OctopoleRFPeak 750 V. The UV detection was carried out in the spectrum range from 190 to 640 nm with a spectrum step of 2 nm. The structural characterization of drugs and their degradants was achieved through collision induced dissociation experiments using collision energies of 20 and 35 eV.

Sample Preparation. Forced degradation studies were performed on the bulk drugs. For each drug, 1.5 mL stock solutions at a concentration of 1.0 mg/mL in ACN/H₂O (50:50; v/v %) were prepared. The stock solutions (1.5 mL) were then diluted with 1.5 mL of 2 M NaOH, 2 M HCl, H₂O, or 30% H₂O₂ (w/w) to promote basic, acidic, neutral hydrolysis, and oxidative degradation, respectively. All the experiments were carried out at 60 °C in the dark, under magnetic stirring. All solutions employed in the different experimental conditions were previously heated at 60 °C in a water bath before use. Olaparib degradations were studied in the time range of 360 min and the samplings (0.1 mL) were carried out at the time points of 0, 5, 10, 15, 30, 60, 180, 270, and 360 min. The acidic hydrolysis of rucaparib and the hydrolysis of niraparib in an alkaline and acidic environment were performed at 48 h with sampling (0.1 mL) at 0, 6, 24, 30, and 48 h. Instead, the basic hydrolysis of rucaparib and the oxidative stress condition for both two drugs were monitored for up to 360 min with sampling (0.1 mL) at 0, 15, 30, 60, 120, and 360 min. Each basic, acidic, and oxidative degradation sample (0.1 mL) was neutralized with HCl, NaOH, and MnO₂, respectively. All samples were filtered through a 0.22 μm membrane filter and diluted to a concentration of 10 $\mu\text{g}/\text{mL}$ (olaparib), 7 $\mu\text{g}/\text{mL}$ (rucaparib), and 1 $\mu\text{g}/\text{mL}$ (niraparib) using a mixture of ACN/H₂O (50:50; v/v %) and analyzed by UHPLC-HRMS analysis.

For the in-depth analysis of basic hydrolysis of olaparib, three different olaparib stock solutions were prepared at the concentration of 1.0 mg/mL using ACN/H₂O (50:50; v/v %), ACN/H₂O (25:75; v/v %), and H₂O (100%) to perform an in-depth study of the basic hydrolysis of olaparib on the bulk drug. Each stock solution (1.5 mL) was diluted with 1.5 mL of 2 M NaOH to promote the degradation to achieve the desired final experimental conditions. All the experiments were performed using the same experimental procedure aforementioned for the forced degradation of olaparib.

ASSOCIATED CONTENT

Supporting Information

The Supporting Information is available free of charge at <https://pubs.acs.org/doi/10.1021/acsomega.2c07815>.

Manual characterization of the product ions of rucaparib DPs, MCS settings, chromatogram of forced basic degradation of olaparib, MoKa prediction of the pKa value, degradation products of rucaparib reported in literature, trend of UV signals in rucaparib and niraparib stress tests, chromatogram of forced oxidative degradation of rucaparib, extracted ion chromatogram, trend of MS and UV signals of Imp-C, MS/MS spectrum of Imp-C and fragment ion interpretation, collection of olaparib and rucaparib degradation studies reported in literature, IUPAC names and mass error of identified DPs, static dielectric constants of ACN:H₂O mixtures, and summary of substrate degradation and extend of DP formation (PDF)

AUTHOR INFORMATION

Corresponding Author

Laura Goracci – Department of Chemistry, Biology and Biotechnology, University of Perugia, 06123 Perugia, Italy;  orcid.org/0000-0002-9282-9013; Email: laura.goracci@unipg.it

Authors

Stefano Bonciarelli – Department of Chemistry, Biology and Biotechnology, University of Perugia, 06123 Perugia, Italy;  orcid.org/0000-0003-0474-0922

Jenny Desantis – Department of Chemistry, Biology and Biotechnology, University of Perugia, 06123 Perugia, Italy;  orcid.org/0000-0002-2334-934X

Simone Cerquiglini – Department of Chemistry, Biology and Biotechnology, University of Perugia, 06123 Perugia, Italy;  orcid.org/0000-0002-3836-7276

Complete contact information is available at:

<https://pubs.acs.org/10.1021/acsomega.2c07815>

Author Contributions

All the authors performed the conceptualization of the research work; sample preparation, optimization of the UHPLC and HRMS conditions, acquisition of UHPLC-HRMS and UHPLC-DAD data, and data analysis with MCS software were performed by S.B.; J.D. synthesized the reference compounds and contributed to data interpretation; S.C. contributed to UHPLC-HRMS method optimization and data acquisition; and L.G. coordinated the project and defined data analysis and interpretation workflow. All authors contributed to the writing of the manuscript. All authors have read and agreed to the published version of the manuscript.

Notes

The authors declare no competing financial interest.

ACKNOWLEDGMENTS

The authors are grateful to the Università degli Studi di Perugia and MIUR for financial support through the project AMIS-“Dipartimenti di Eccellenza-2018–2022”.

REFERENCES

- (1) Melo, S. R.; Homem-de-Mello, M.; Silveira, D.; Simeoni, L. A. Advice on Degradation Products in Pharmaceuticals: A Toxicological Evaluation. *PDA J. Pharm. Sci. Technol.* **2014**, *68*, 221–238.
- (2) Alsante, K. M.; Ando, A.; Brown, R.; Ensing, J.; Hatajik, T. D.; Kong, W.; Tsuda, Y. The role of degradant profiling in active pharmaceutical ingredients and drug products. *Adv. Drug Delivery Rev.* **2007**, *59*, 29–37.
- (3) Singh, S.; Junwal, M.; Modhe, G.; Tiwari, H.; Kurmi, M.; Parashar, N.; Sidduri, P. Forced degradation studies to assess the stability of drugs and products. *TrAC, Trends Anal. Chem.* **2013**, *49*, 71–88.
- (4) Görög, S. Drug safety, drug quality, drug analysis. *J. Pharm. Biomed. Anal.* **2008**, *48*, 247–253.
- (5) Blessy, M.; Patel, R. D.; Prajapati, P. N.; Agrawal, Y. K. Development of forced degradation and stability indicating studies of drugs-A review. *J. Pharm. Anal.* **2014**, *4*, 159–165.
- (6) Qiu, F.; Norwood, D. L. Identification of Pharmaceutical Impurities. *J. Liq. Chromatogr. Relat. Technol.* **2007**, *30*, 877–935.
- (7) Wróblewski, K.; Szultka-Młyńska, M.; Janiszewska, D.; Petruczynik, A.; Buszewski, B. Development of the Validated Stability-Indicating Method for the Determination of Vortioxetine in Bulk and Pharmaceutical Formulation by HPLC-DAD, Stress Degradation Kinetics Studies and Detection of Degradation Products by LC-ESI-QTOF-MS. *Molecules* **2022**, *27*, 1883.
- (8) Roberto de Alvarenga Junior, B.; Lajarim Carneiro, R. Chemometrics Approaches in Forced Degradation Studies of Pharmaceutical Drugs. *Molecules* **2019**, *24*, 3804.
- (9) Rajput, N.; Soni, F.; Sahu, A. K.; Jadav, T.; Sharma, S.; Sengupta, P. Degradation kinetics and characterization of major degradants of binimetinib employing liquid chromatography-high resolution mass spectrometry. *J. Pharm. Biomed. Anal.* **2022**, *215*, 114753.
- (10) World Health Organization. *Stability Testing of Active Pharmaceutical Ingredients and Finished Pharmaceutical Products*; Geneva: Switzerland, 2009.
- (11) International Council for Harmonisation of Technical Requirements for Pharmaceuticals for Human Use. *Stability Testing of New Drug Substances and Products Q1A(R2)*; Geneva, Switzerland, 2000.
- (12) Janzen, H. Forced degradation studies -comparison between ICH, EMA, FDA and WHO guidelines and ANVISA's resolution RDC 53/2015. Master Dissertation, Universität Bonn, 2015.
- (13) Bakshi, M.; Singh, S. Development of validated stability-indicating assay methods-critical review. *J. Pharm. Biomed. Anal.* **2002**, *28*, 1011–1040.
- (14) Lopez-Ruiz, R.; Romero-González, R.; Ortega-Carrasco, E.; Martínez Vidal, J. L.; Garrido Frenich, A. Degradation studies of dimethylchlor in soils and water by UHPLC-HRMS: putative elucidation of unknown metabolites. *Pest Manage. Sci.* **2020**, *76*, 721–729.
- (15) Bonciarelli, S.; Desantis, J.; Goracci, L.; Siragusa, L.; Zamora, I.; Ortega-Carrasco, E. Automatic Identification of Lansoprazole Degradants under Stress Conditions by LC-HRMS with MassChemSite and WebChembase. *J. Chem. Inf. Model.* **2021**, *61*, 2706–2719.
- (16) Hughes, D. L. Patent Review of Manufacturing Routes to Recently Approved PARP Inhibitors: Olaparib, Rucaparib, and Niraparib. *Org. Process Res. Dev.* **2017**, *21*, 1227–1244.
- (17) Deeks, E. D. Olaparib: first global approval. *Drugs* **2015**, *75*, 231–240.
- (18) Balasubramaniam, S.; Beaver, J. A.; Horton, S.; Fernandes, L. L.; Tang, S.; Horne, H. N.; Liu, J.; Liu, C.; Schrieber, S. J.; Yu, J.; Song, P.; Pierce, W.; Robertson, K. J.; Palmby, T. R.; Chiu, H. J.; Lee, E. Y.; Philip, R.; Schuck, R.; Charlab, R.; Banerjee, A.; Chen, X. H.; Wang, X.; Goldberg, K. B.; Sridhara, R.; Kim, G.; Pazdur, R. FDA Approval Summary: Rucaparib for the Treatment of Patients with Deleterious BRCA Mutation-Associated Advanced Ovarian Cancer. *Clin. Cancer Res.* **2017**, *23*, 7165–7170.
- (19) Valabrega, G.; Scotto, G.; Tuninetti, V.; Pani, A.; Scaglione, F. Differences in PARP Inhibitors for the Treatment of Ovarian Cancer: Mechanisms of Action, Pharmacology, Safety, and Efficacy. *Int. J. Mol. Sci.* **2021**, *22*, 4203.
- (20) Thummar, M.; Kuswah, B. S.; Samanthula, G.; Bulbake, U.; Gour, J.; Khan, W. Validated stability indicating assay method of olaparib: LC-ESI-Q-TOF-MS/MS and NMR studies for characterization of its new hydrolytic and oxidative forced degradation products. *J. Pharm. Biomed. Anal.* **2018**, *160*, 89–98.
- (21) Kallepalli, P.; Annapurna, M. Separation, Identification and Quantification of process related Impurities and Stress Degradants of Olaparib by LC-ESI-Q-TOF-MS. *Res. J. Pharm. Technol.* **2018**, *11*, 3718.
- (22) Khedr, A.; El-Hay, S. S. A.; Kammoun, A. K. Multi-Steps Fragmentation-Ion Trap Mass Spectrometry Coupled to Liquid Chromatography Diode Array System for Investigation of Olaparib Related Substances. *Molecules* **2019**, *24*, 843.
- (23) Kavitapu, D.; Maruthapillai, A.; Devikala, S.; Selvi, J. A.; Tamilselvi, M.; Mahapatra, S.; Kumar, G. P.; Tyagi, P. K. New Rapid Stability indicating RP-UPLC Method for the Determination of Olaparib, its Related Substances and Degradation Products in Bulk drug and Dosage Form. *Mater. Today: Proc.* **2019**, *14*, 492–503.
- (24) Palakeeti, B.; Ramesh, T.; Reddy, K. V.; Konakanchi, R.; Rao, P. N.; Gobi, K. V. Identification and Characterisation of Rucaparib Degradation Products and Their Comparison with Known Impurities. *Chromatographia* **2018**, *82*, 591–604.

- (25) Suchitra, D.; Battu, S. A Stability Indicating Reverse Phase-HPLC Method Development and Validation for the Estimation of Rucaparib in Bulk and Pharmaceutical Dosage Form. *Am. J. Anal. Chem.* **2021**, *12*, 96–107.
- (26) Zhou, D.; Porter, W. R.; Zhang, G. G. Z.; Qiu, Y. Chapter 5—Drug Stability and Degradation Studies. In *Developing Solid Oral Dosage Forms*, 2nd ed.; Chen, Y., Zhang, G. G. Z., Yu, L., Mantri, R. V., Eds.; Academic Press: Boston, 2017; pp 113–149.
- (27) Bairagi, S. M.; Gunupudi, P.; Abbaraju, V.; Srinivas, R.; Talluri, M. V. N. K. Study of forced degradation behaviour of cobicistat and atazanavir using LC/ESI/QTOF/MS; Combination of in-sourced and collision-induced dissociation for evaluation of the fragmentation patterns of degradation products. *New J. Chem.* **2018**, *42*, 19113.
- (28) Bairagi, S. M.; Srinivas, R.; Talluri, M. V. N. K. Identification and structural characterization of hydrolytic degradation products of alvimopan by LC/QTOF/MS/MS and NMR studies. *J. Pharm. Biomed. Anal.* **2019**, *165*, 399–409.
- (29) Udutha, S.; Shankar, G.; Borkar, R. M.; Kumar, K.; Srinivasulu, G.; Guntuku, L.; Naidu, V. G. M.; Srinivas, R. Identification and characterization of stress degradation products of sumatriptan succinate by using LC/Q-TOF-ESI-MS/MS and NMR: Toxicity evaluation of degradation products. *J. Mass Spectrom.* **2018**, *53*, 963–975.
- (30) Menear, K. A.; Adcock, C.; Boulter, R.; Cockcroft, X. L.; Copsey, L.; Cranston, A.; Dillon, K. J.; Drzewiecki, J.; Garman, S.; Gomez, S.; Javaid, H.; Kerrigan, F.; Knights, C.; Lau, A.; Loh, V. M., Jr.; Matthews, I. T.; Moore, S.; O'Connor, M. J.; Smith, G. C.; Martin, N. M. 4-[3-(4-cyclopropanecarbonylpiperazine-1-carbonyl)-4-fluorobenzyl]-2H-phthalazin-1-one: a novel bioavailable inhibitor of poly(ADP-ribose) polymerase-1. *J. Med. Chem.* **2008**, *51*, 6581–6591.
- (31) Zhang, J.; Wu, H.; Kim, E.; El-Shourbagy, T. A. Salting-out assisted liquid/liquid extraction with acetonitrile: a new high throughput sample preparation technique for good laboratory practice bioanalysis using liquid chromatography–mass spectrometry. *Biomed. Chromatogr.* **2009**, *23*, 419–425.
- (32) Parker, A. J. Protic-dipolar aprotic solvent effects on rates of bimolecular reactions. *Chem. Rev.* **1969**, *69*, 1–32.
- (33) Roberts, D. D. Solvent Effects. III. The Influence of Aqueous Dimethyl Sulfoxide on Alkyl Benzoate Ester Saponification Reactions. *J. Org. Chem.* **1966**, *31*, 4037–4041.
- (34) Khan, M. N. Salt and solvent effects on alkaline hydrolysis of N-hydroxyphthalimide. Kinetic evidence for ion-pair formation. *J. Phys. Org. Chem.* **1994**, *7*, 412–419.
- (35) Ye, C. M.; Ariffin, A.; Khan, M. N. Solvent Effects On Alkaline Hydrolysis Of N-Benzylphthalimide In Mixed Water-Acetonitrile And Mixed Water-N,N-Dimethylformamide. *Indian J. Chem., Sect. A: Inorg., Bio-inorg., Phys., Theor. Anal. Chem.* **2005**, *44*, 2055–2059.
- (36) Leng, S. Y.; Ariffin, A.; Khan, M. N. Effects of mixed aqueous-organic solvents on the rate of intramolecular carboxylic group-catalyzed cleavage of N-(4'-methoxyphenyl)phthalimide acid. *Int. J. Chem. Kinet.* **2004**, *36*, 316–325.
- (37) Milletti, F.; Storchi, L.; Sforza, G.; Cruciani, G. New and Original pKa Prediction Method Using Grid Molecular Interaction Fields. *J. Chem. Inf. Model.* **2007**, *47*, 2172–2181.
- (38) Amis, E. S. Coulomb's law and the quantitative interpretation of reaction rates. *J. Chem. Educ.* **1952**, *29*, 337.
- (39) Grützmacher, H.-F. Fragmentation in Mass Spectrometry. In *Encyclopedia of Spectroscopy and Spectrometry*; Lindon, J. C., Ed.; Elsevier: Oxford, 1999; pp 637–648.

□ Recommended by ACS

A Robust Purity Method for Biotherapeutics Using New Peak Detection in an LC–MS-Based Multi-Attribute Method

Monica Sadek, Galahad Deperalta, et al.

FEBRUARY 21, 2023

JOURNAL OF THE AMERICAN SOCIETY FOR MASS SPECTROMETRY

READ ↗

Targeted Small-Molecule Identification Using Heartcutting Liquid Chromatography–Infrared Ion Spectroscopy

Rianne E. van Outersterp, Jonathan Martens, et al.

FEBRUARY 03, 2023

ANALYTICAL CHEMISTRY

READ ↗

DART-MS Facilitated Quantification of Cannabinoids in Complex Edible Matrices—Focus on Chocolates and Gelatin-Based Fruit Candies

Megan I. Chambers, Rabi A. Musah, et al.

APRIL 10, 2023

ACS OMEGA

READ ↗

Introducing “DoPP”: A Graphical User-Friendly Application for the Rapid Species Identification of Psychoactive Plant Materials and Quantification of Psychoactive Small Mole...

Samira Beyramysoltan, Rabi A. Musah, et al.

NOVEMBER 17, 2022

ANALYTICAL CHEMISTRY

READ ↗

Get More Suggestions >